ChemComm

Accepted Manuscript

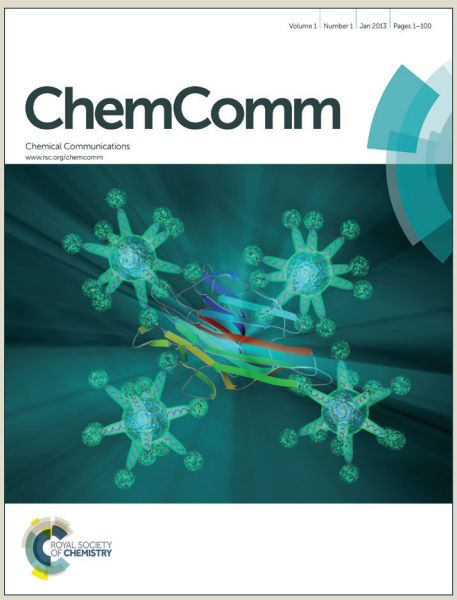

ROYAL SOCIETY OF CHEMISTRY

www.rsc.org/chemcomm

Journal Name

RSCPublishing

COMMUNICATION

Chemical Reaction-Induced Multi-molecular Polarization (CRIMP)

Cite this: DOI: 10.1039/x0xx00000x

Y. Lee,[a‡] N.M. Zacharias,[b‡] D. Piwnica-Worms,[b] P. K. Bhattacharya[b*]

Received 00th January 2012,
Accepted 00th January 2012

DOI: 10.1039/x0xx00000x
www.rsc.org/

Here we present a novel hyperpolarization method, Chemical Reaction-Induced Multi-molecular Polarization (CRIMP), which could be applied to the study of several *in vivo* processes simultaneously including glycolysis, TCA cycle, fatty acid synthesis and pH mapping. Through the use of non-enzymatic decarboxylation, we generate four hyperpolarized imaging agents from hyperpolarized 1,2-^{13}C pyruvic acid.

Solid-to-liquid state Dynamic Nuclear Polarization (DNP) can achieve a large enhancement of magnetic resonance (MR) signal with small organic compounds, including biological metabolites. With this signal enhancement, traditionally insensitive low-gamma nuclei, as well as nuclei with low natural abundance, such as ^{13}C and ^{15}N, can be observed directly without extensive signal averaging.[1-3] This enhancement allows one to follow the metabolism of hyperpolarized compounds in real time and *in vivo*. Metabolism is fundamental to the cell and is significantly altered in many diseases, such as cancer, neurodegeneration, diabetes and cardiac dysfunction.[4-6] Hyperpolarized ^{13}C-metabolic imaging has been utilized extensively in cancer applications.[5, 7, 8] However, despite advantages of this new emerging technique, applicability of the hyperpolarization technique has been generally limited in clinical settings to studying glycolysis through the use of hyperpolarized pyruvate. In addition, several practical restrictions arise for *in vivo* applications using direct hyperpolarization of most organic compounds because of low solubility in aqueous media and insufficient DNP signal enhancement. Here, we propose a new hyperpolarization-based methodology, namely Chemical Reaction-Induced Multi-molecular Polarization (CRIMP). Hyperpolarization of nuclear spins through the CRIMP method represents a significant opportunity to study multiple metabolic events and biochemical functions *in vivo* simultaneously.

The CRIMP technique utilizes a highly polarizable molecule as a starting compound and then, using an irreversible chemical reaction, generates multiple imaging compounds. Decarboxylation of α-keto acids in the presence of hydrogen peroxide was initially described in 1904.[9] The ability of pyruvate to quench hydrogen peroxide has been shown to protect both neurons and other cells types from hydrogen peroxide-induced toxicity.[10, 11] Highly polarizable pyruvic acid reacts instantly and irreversibly with hydrogen peroxide resulting in generation of acetate and carbon dioxide. During the chemical reaction, the spin polarization is transferred from the hyperpolarized 1,2-^{13}C-pyruvate to the reaction products, 1-^{13}C acetate and carbon dioxide ($^{13}CO_2$) (Scheme 1).

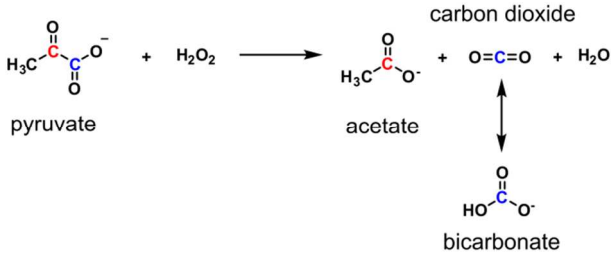

Scheme 1. Non-enzymatic decarboxylation reaction between pyruvate and hydrogen peroxide for Chemical Reaction-Induced Multi-molecular Polarization (CRIMP).

Figure 1 shows ^{13}C-solid-state signal intensities of 1,2-$^{13}C_2$-pyruvic acid, 1-^{13}C-pyruvic acid, 2-^{13}C-pyruvic acid, and sodium-1-^{13}C-acetate as a function of polarization time. 1 mM gadolinium (III) relaxation agent (ProHance, Bracco Diagnostic Inc.) (optimal concentration for the DNP process; data not shown here) was added into each sample for greater solid-state polarization enhancement. Polarization is achieved by placing the mixture in a sample cup that is inserted into a DNP HyperSense polarizer (Oxford Instuments, Tubney Woods, UK) where it is irradiated at a 100 mW power of 94.124 GHz (ω_e - ω_N) microwave frequency at a temperature of 1.4 K (Figure 1 and Supporting Information). The solid state polarization build-up is measured with small pulses every 5 minutes, and after polarization plateau (Figure 1), the frozen sample is dissolved in superheated solvent and injected either into an animal or used as a phantom in an MR scanner. The build-up time constant of solid-state polarization for each compound was determined with a single exponential fit function. All pyruvic acid samples showed fast solid-state polarization build-up time constants (~ 700 s), while the sodium acetate showed a four times longer solid-state build-up rate

constant (~ 2,800 s) than pyruvic acid. Signal intensity of the double labeled pyruvic acid in the solid-state showed a value similar to the sum of the intensities of the two single labeled pyruvic acids.

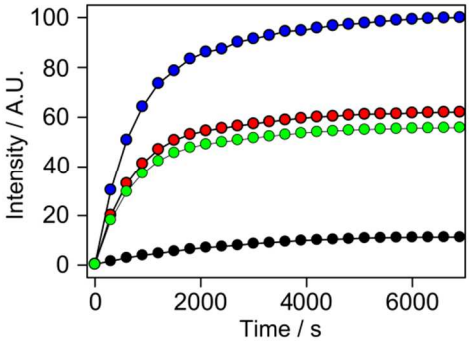

Figure 1. Curves showing solid-state polarization build-up progression over time of 1,2-$^{13}C_2$-pyruvic acid (blue color), 1-^{13}C-pyruvic acid(red color), 2-^{13}C-pyruvic acid (green color), 5 M sodium 1-^{13}C-acetate (black color) in a 60%:40% (v/v) glycerol/water glassing agent with 15 mM OX063 free radical and 1 mM gadolinium (III) relaxation agent (ProHance, Bracco Diagnostic Inc.). The data points were normalized to unit intensity.

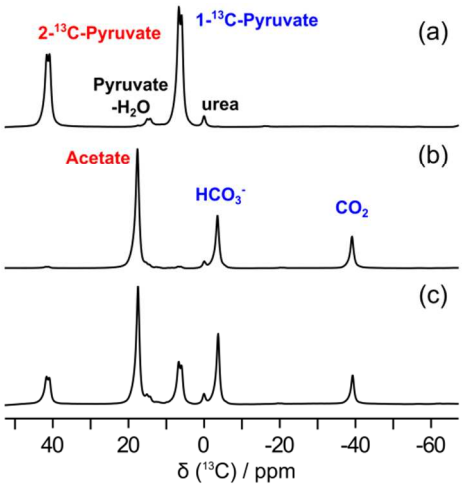

Figure 2. (a) Hyperpolarized ^{13}C magnetic resonance spectrum of 1,2-$^{13}C_2$-pyruvate. (b) Reaction with H_2O_2 (full conversion). (c) Reaction with H_2O_2 (partial conversion).

Figure 2 represents hyperpolarized spectra of 1,2-$^{13}C_2$-pyruvate (Figure 2a: reference, Figure 2b-c: reaction with hydrogen peroxide). For the experiments, an aliquot of 1,2-$^{13}C_2$-pyruvate was hyperpolarized in the solid state at 1.4 K, and rapidly dissolved in buffered solution heated to ~180 °C under pressure. For the CRIMP method, varying amounts of hydrogen peroxide (10 µl ~ 30 µl) were preloaded in the sample reactor, and gently mixed with the hyperpolarized pyruvate solution after dissolution. Magnetic resonance measurement was triggered 25 ~ 30 s after dissolution. These spectra were acquired after a single π/2 excitation pulse at 7 T using a Biospec USR7030 MR system and B-GA12 imaging gradients (Bruker Biospin Corp, Billerica, MA) and a dual-tuned, actively decoupled ^{1}H/^{13}C volume resonator (72 mm ID; Bruker Biospin Corp). As represented in Figure 2b, hyperpolarized 1,2-$^{13}C_2$-pyruvate (C1: 6.2 ppm, C2: 41.1 ppm) was fully converted to hyperpolarized 1-^{13}C-acetate (17.4 ppm), $H^{13}CO_3^-$ (-3.7 ppm) and $^{13}CO_2$ (-39.3 ppm) in the presence of excess amounts of hydrogen peroxide[12]. As shown in Figure 2c, progress of the reaction can readily be controlled by changing the concentration of hydrogen peroxide, resulting in the generation of multiple hyperpolarized imaging agents for glycolysis (1-^{13}C-pyruvate), energy metabolism (1-^{13}C-acetate), and *in vivo* pH mapping ($H^{13}CO_3^-$ and $^{13}CO_2$) from the single hyperpolarized agent, 1,2-$^{13}C_2$-pyruvate.

It is important in the CRIMP method that the reaction is complete prior to injection of the multiple component imaging compounds. If this were not the case, it would be difficult to determine whether resonances seen *in vivo* were occurring due to metabolism or the continuation of the CRIMP reaction. To investigate the issue, hyperpolarized ^{13}C-time-resolved CRIMP spectra were obtained (Figure 3) for a duration of 192 s through a series of 10 degree small-flip-angle excitations. Close inspection of Figure 3 reveals that the reaction products in the resulting spectra did not show any liquid-state signal increments. Moreover, the spin-lattice relaxation time of 1,2-$^{13}C_2$-pyruvate determined from the CRIMP method agreed to 10 ± 2 % with reference rate constants determined from single compound polarization. Therefore, it is reasonable to presume that the decarboxylation reaction is complete during the delay time and mixing time prior to the sample being placed in the scanner. Spin-lattice relaxation times and polarizations level of these compounds after dissolution are summarized in Table 1.

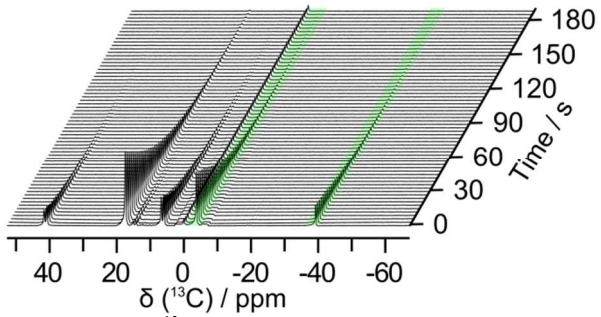

Figure 3. Series of ^{13}C magnetic resonance spectra recorded from a single sample of hyperpolarized 1,2-$^{13}C_2$-pyruvate mixed with H_2O_2. Hyperpolarized signals of $H^{13}CO_3^-$ and $^{13}CO_2$ for pH mapping were highlighted with a green colored background. These spectra were acquired using 64 sequential transients 10° pulses (Supporting Information).

In addition to simple determination of spin-lattice relaxation times and polarization levels from the CRIMP method, we wanted to determine if hyperpolarized $^{13}CO_2$ and $H^{13}CO_3^-$ generated by the method could be utilized to calculate bulk *in vivo* pH, expressed in the form of the concentration ratio between bicarbonate and carbon dioxide from the Henderson-Hasselbalch equation (eq 1).

$$pH = pKa + \log_{10}([HCO_3^-]/[CO_2]) \quad (1)$$

where *pKa* (logarithmic constant) is known to be 6.17 *in vivo*[13]. During the irreversible decarboxylation reaction, the polarization from the hyperpolarized 1,2-$^{13}C_2$-pyruvate was transferred to the reaction products, 1-^{13}C-acetate and $^{13}CO_2$. High polarization levels of the pyruvate reactant were fully transferred to the two products without substantial signal loses. Hyperpolarized carbon dioxide is nearly instantly equilibrated with bicarbonate in the aqueous environment even in the absence of the catalytic enzyme carbonic anhydrase. Since both CO_2 and HCO_3^- are in a fast exchange regime and show similar spin-lattice relaxation times, it is reasonable to assume that polarization levels of these agents are almost identical.[13, 14] Under this condition, the pH values can be simply calculated from the signal intensity ratio of the two exchangeable products. The calculated pH value was fairly consistent over 100 s after the

reaction and mixing time (Supporting Information). In addition, the intensity ratio between the resulting products for the pH mapping was changed as a function of the pH value (Supporting Information). Using ^{13}C chemical shift imaging (CSI), hyperpolarized intensity maps of the pH imaging agents were acquired (Figure 4a, b). The pH calculated from the ratio corresponded to the pH within $\pm$ 0.5 units determined directly by a conventional pH meter (Supporting Information). The absolute pH difference was not precisely investigated here, but this difference is likely due to the presence of residual unreacted pyruvic acid in the media after the reaction.

Table 1. Summary of longitudinal relaxations times (T_1) and polarization levels

Method	Compound	T_1 (s)†	*Polarization Level (%)
Reference	1,2-$^{13}C_2$ Pyruvate (C1)	40 ± 2	18 ± 3
	1,2-$^{13}C_2$ Pyruvate (C2)	35 ± 2	12 ± 3
	1-^{13}C Na-Acetate	50 ± 1	16 ± 2
CRIMP	Acetate	54 ± 1	11 ± 3
	$H^{13}CO_3^-$	42 ± 2	5**
	$^{13}CO_2$	44 ± 3	3**

† To obtain the spin-lattice relaxation time from the CRIMP data, a series of fixed small-flip-angle pulses were applied to acquire magnetic resonance spectra at equal time intervals. To account for the depletion of polarization by these pulses, a single exponential relaxation equation was multiplied by the factor $e^{-\lambda \cdot t}$ prior to calculating the T_1 relaxation time. In the exponential, $\lambda = -\ln[\cos(\alpha)]/\Delta t$ depends on the flip angle (α) and the time interval (Δt) between magnetic resonance acquisitions. *Liquid state polarization percentages were determined 25 – 30 s after dissolution using an 8 M 1-^{13}C urea phantom as a standard. ** Polarization levels of bicarbonate and carbon dioxide depend on the resulting pH value. Standard deviations of the T_1 and polarization level are reported ($N = 3$).

Conclusions

The CRIMP method is a simple versatile chemical method that can be done without any physical changes to the dissolution pathway or to the polarizer. Many new techniques in the literature including cross polarization[15], microwave frequency modulation[16, 17], generating a faster dissolution or injection setup[18] and increasing the magnetic field from dissolution to scanner[19, 20] are all physical methods used to increase hyperpolarization percentages or to increase the T_1 value of hyperpolarized imaging compounds. Other labs use chemical techniques such as generating water soluble salts of compounds to increase hyperpolarization percentages or increase the concentration of the compound[13, 21]. However, many of these complex-salts require an ion-exchange column after dissolution to remove the salt.

In addition in this iteration of the CRIMP method, we utilize the "gold" standard hyperpolarized molecule pyruvic acid. The high polarization percentage and long T_1 of pyruvate have allowed this compound to be the first hyperpolarized agent used in the clinic[22]. The clinical DNP polarizer (SpinLab™) built by General Electric is made specifically for the polarization of pyruvic acid. The polarization percentages we have achieved with the HyperSense will significantly increase if the work was done using the SpinLab™, which utilizes a stronger magnetic field and a lower temperature in the DNP process.

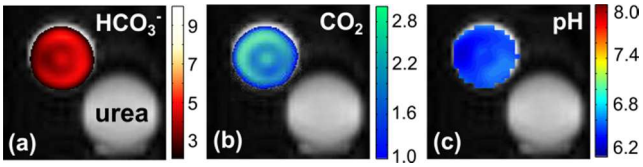

Figure 4. Chemical shift intensity maps of phantom containing hyperpolarized (a) $H^{13}CO_3^-$ and (b) $^{13}CO_2$. (c) pH map calculated from the ratio of intensity of $H^{13}CO_3^-$ and $^{13}CO_2$.

Table 2. Advantages of CRIMP Method

Features	Multi-compound polarization	CRIMP
Polarization Build-up Rate	Slow	Fast
Polarization Level	5-10%	18%
Solubility Limit in Preparation of Sample	1.5-5 M	14 M
Microwave Offset Problem	+	N/A
Solid-state Sample Volume Problem	+	20 µl*

*Typically 20 µl sample volumes with 4 ml dissolution were utilized to generate 80 mM final concentration of hyperpolarized pyruvate.

The ability to generate multi-component polarizations from a hyperpolarized single component via chemical reaction provides several advantages over multi-compound polarization (Table 2).[14] In this iteration, the chemical reaction approach has the following distinct advantages over multi-compound polarization, **(1)** utilizes the high solid-state polarization of pyruvic acid. 1,2-$^{13}C_2$-pyruvic acid can be hyperpolarized routinely to 18 %. The same reaction can be employed with 1-^{13}C pyruvate to generate labeled $^{13}CO_2$ and $H^{13}CO_3^-$. We can also consistently hyperpolarize 1-^{13}C pyruvic acid to 30%. Systematic improvements to allow for fast and homogeneous mixing of the hyperpolarized agent and hydrogen peroxide may further expand the scope of these results. **(2)** Makes use of the faster polarization build-up rate of pyruvic acid. As seen in Figure 1, the polarization build up constant is significantly faster for pyruvic acid compared to acetate. **(3)** Minimizes signal loses during sample transfer. Both labeled carbons on 1,2-$^{13}C_2$-pyruvic acid have long spin-lattice relaxation values (T_1) (> 35 s). We can therefore perform CRIMP right in front of MR scanner after dissolution of hyperpolarized pyruvic acid. **(4)** Traverses off-resonance effects on the microwave frequency. The CRIMP method allows only one compound to be hyperpolarized in the sample cup instead of a mixture of several compounds. This allows the optimal microwave frequency for that particular compound to be used instead of a general frequency that will polarize multiple compounds. **(5)** Allows for higher final concentrations of polarized compounds. Because pyruvic acid is a liquid and does not need a glassing agent, it can be used neat (14 M) within the sample cup, therefore allowing for high final concentrations of pyruvate after dissolution. This is significantly higher than for acetate (sodium acetate 1.0 – 4.5 M),[15, 23] for sodium bicarbonate (1.69 M)[14] or cesium bicarbonate (6.8 M)[13]. We see complete conversion of

pyruvic acid to acetate and carbon dioxide. However because the reaction is performed open to the atmosphere, there is loss of a percentage of carbon dioxide gas after each reaction.

Future studies utilizing other fast reactions with ^{13}C and ^{15}N labeled compounds are being explored. This reaction could be used with any α-keto acid. For instance, multi-labeled ^{13}C α-ketoglutaric would generate propanoic acid and bicarbonate. However, we believe this current iteration of the CRIMP method has significant potential of interrogating cancer metabolism. We are utilizing this technique to generate 1-^{13}C hyperpolarized acetate reproducibly with hyperpolarized 1-^{13}C pyruvate to navigate the activities of acetyl-CoA synthetase and lactate dehydrogenase simultaneously. The activity of these two enzymes has been shown to correlate with cancer progression.[24-28] In the case of acetate, radioactive ^{11}C-acetate and ^{18}F-acetate uptake has been utilized in the detection of cancer.[26-28] Co-injection of hyperpolarized acetate and pyruvate potentially allows for glycolysis, fatty acid synthesis and the TCA cycle metabolism to be interrogated simultaneously employing non-radioactive stable isotope-labeled compounds. In summary, using DNP-enhanced magnetic resonance spectroscopy and imaging, the chemical reaction-induced multi-component polarization method has been demonstrated. The new method can potentially be applied to study several *in vivo* metabolic pathways and multiple biochemical reactions concurrently in real-time.

Notes and references

[a] Hanyang University, Department of Applied Chemistry, Ansan, 426-791, Korea.

[b] University of Texas MD Anderson Cancer Center, Department of Cancer Systems Imaging, Houston, TX 77030.

‡ These authors contributed equally. * Corresponding author.
pkbhattacharya@mdanderson.org

Electronic Supplementary Information (ESI) available: Experimental section, Supplementary figures. See DOI: 10.1039/c000000x/

1. J. H. Ardenkjaer-Larsen, B. Fridlund, A. Gram, G. Hansson, L. Hansson, M. H. Lerche, R. Servin, M. Thaning and K. Golman, *Proc Natl Acad Sci U S A*, 2003, **100**, 10158-10163.
2. J. H. Ardenkjaer-Larsen, H. Johannesson, J. S. Petersson and J. Wolber, *Methods Mol Biol*, 2011, **771**, 655-689.
3. K. Golman, J. H. Ardenkjaer-Larsen, J. S. Petersson, S. Mansson and I. Leunbach, *Proc Natl Acad Sci U S A*, 2003, **100**, 10435-10439.
4. P. Bhattacharya, B. D. Ross and R. Bunger, *Exp Biol Med (Maywood)*, 2009, **234**, 1395-1416.
5. R. E. Hurd, Y. F. Yen, A. Chen and J. H. Ardenkjaer-Larsen, *J Magn Reson Imaging*, 2012, **36**, 1314-1328.
6. P. Bhattacharya, E. Y. Chekmenev, W. H. Perman, K. C. Harris, A. P. Lin, V. A. Norton, C. T. Tan, B. D. Ross and D. P. Weitekamp, *J Magn Reson*, 2007, **186**, 150-155.
7. S. J. Nelson, J. Kurhanewicz, D. B. Vigneron, P. E. Larson, A. L. Harzstark, M. Ferrone, M. van Criekinge, J. W. Chang, R. Bok, I. Park, G. Reed, L. Carvajal, E. J. Small, P. Munster, V. K. Weinberg, J. H. Ardenkjaer-Larsen, A. P. Chen, R. E. Hurd, L. I. Odegardstuen, F. J. Robb, J. Tropp and J. A. Murray, *Sci Transl Med*, 2013, **5**, 198ra108.
8. K. Brindle, *Br J Radiol*, 2012, **85**, 697-708.
9. M. A. F. Hollerman, *Recl Trav Chim Pays Bas,* 1904, **23**, 169-171.
10. S. Desagher, J. Glowinski and J. Premont, *J Neurosci*, 1997, **17**, 9060-9067.
11. A. Shostak, L. Gotloib, R. Kushnier and V. Wajsbrot, *Nephron*, 2000, **84**, 362-366.
12. H. Zeng, Y. Lee and C. Hilty, *Anal Chem*, 2010, **82**, 8897-8902.
13. F. A. Gallagher, M. I. Kettunen, S. E. Day, D. E. Hu, J. H. Ardenkjaer-Larsen, R. Zandt, P. R. Jensen, M. Karlsson, K. Golman, M. H. Lerche and K. M. Brindle, *Nature*, 2008, **453**, 940-943.
14. D. M. Wilson, K. R. Keshari, P. E. Larson, A. P. Chen, S. Hu, M. Van Criekinge, R. Bok, S. J. Nelson, J. M. Macdonald, D. B. Vigneron and J. Kurhanewicz, *J Magn Reson*, 2010, **205**, 141-147.
15. B. Vuichoud, J. Milani, A. Bornet, R. Melzi, S. Jannin and G. Bodenhausen, *J Phys Chem B*, 2014, **118**, 1411-1415.
16. S. Jannin, A. Bornet, J. Milani, B. Vuichoud, A. J. Perez-Linde and G. Bodenhausen, *Experimental Nuclear Magnetic Resonance Conference May 23-28 2014, Poster 010.* , 2014.
17. M. C. Cassidy, H. R. Chan, B. D. Ross, P. K. Bhattacharya and C. M. Marcus, *Nat Nanotechnol*, 2013, **8**, 363-368.
18. T. Cheng, M. Mishkovsky, J. A. Bastiaansen, O. Ouari, P. Hautle, P. Tordo, B. van den Brandt and A. Comment, *NMR Biomed*, 2013, **26**, 1582-1588.
19. J. Milani, B. Vuichoud, A. Bornet, S. Jannin and G. Bodenhausen, *Experimental Nuclear Magnetic Resonance Conference May 23-28 2014, Poster 011.*, 2014.
20. P. Mieville, S. Jannin and G. Bodenhausen, *J Magn Reson*, 2011, **210**, 137-140.
21. S. Bowen and J. H. Ardenkjaer-Larsen, *J Magn Reson*, 2013, **236**, 26-30.
22. S. J. Nelson, J. Kurhanewicz, D. B. Vigneron, P. E. Larson, A. L. Harzstark, M. Ferrone, M. van Criekinge, J. W. Chang, R. Bok, I. Park, G. Reed, L. Carvajal, E. J. Small, P. Munster, V. K. Weinberg, J. H. Ardenkjaer-Larsen, A. P. Chen, R. E. Hurd, L. I. Odegardstuen, F. J. Robb, J. Tropp and J. A. Murray, *Sci Transl Med*, 2013, **5**, 198ra108.
23. J. A. Bastiaansen, T. Cheng, M. Mishkovsky, J. M. Duarte, A. Comment and R. Gruetter, *Biochim Biophys Acta*, 2013, **1830**, 4171-4178.
24. K. R. Keshari, R. Sriram, M. Van Criekinge, D. M. Wilson, Z. J. Wang, D. B. Vigneron, D. M. Peehl and J. Kurhanewicz, *Prostate*, 2013, **73**, 1171-1181.
25. C. Stavraka, D. J. Pinato, S. J. Turnbull, M. J. Flynn, M. D. Forster, S. M. O'Cathail, S. Babar, M. J. Seckl, R. S. Kristeleit and S. P. Blagden, *Cancer*, 2014, **120**, 262-270.
26. Y. Yoshii, A. Waki, T. Furukawa, Y. Kiyono, T. Mori, H. Yoshii, T. Kudo, H. Okazawa, M. J. Welch and Y. Fujibayashi, *Nucl Med Biol*, 2009, **36**, 771-777.
27. N. Oyama, H. Okazawa, N. Kusukawa, T. Kaneda, Y. Miwa, H. Akino, Y. Fujibayashi, Y. Yonekura, M. J. Welch and O. Yokoyama, *Eur J Nucl Med Mol Imaging*, 2009, **36**, 422-427.
28. C. L. Ho, M. K. Cheung, S. Chen, T. T. Cheung, Y. L. Leung, K. C. Cheng and W. D. Yeung, *Mol Imaging*, 2012, **11**, 229-239.

